

Analytical and Numerical Solutions for Nonlinear Equations

©Available online at https://ansne.du.ac.ir/ Online ISSN: 3060-785X

2024, Volume 9, Issue 2, pp. 270-279



Research article

On the Nonlinear Equation of State in Black Hole Thermodynamics

Sudhaker Upadhyay*

Department of Physics, K.L.S. College, Nawada, Magadh University, Bodh Gaya, Bihar 805110, India

* Corresponding author(s): sudhakerupadhyay@gmail.com

Received: 16/09/2025 Published: 29/10/2025 Accepted: 13/10/2025



doi 10.22128/ansne.2025.3060.1154

Abstract

The study of black hole thermodynamics has revealed profound connections between gravitation, quantum theory, and statistical mechanics. In many instances, the key physical information is encoded in nonlinear algebraic or transcendental equations that relate horizon radius, temperature, and pressure. In this work we examine a specific nonlinear equation arising from the extended phase space of charged anti-de Sitter (AdS) black holes. By analyzing its structure and obtaining approximate and exact solutions, we highlight the physical implications for the thermodynamic stability of black holes. Our results clarify the role of nonlinearities in determining critical points and phase transitions analogous to the van der Waals fluid.

Keywords: Black hole thermodynamics, Phase transitions, Nonlinear equations

Mathematics Subject Classification (2020): 83C57, 80A10, 35Q75, 34C23

1 Introduction

The discovery of black hole thermodynamics fundamentally altered our understanding of gravity, quantum theory, and statistical mechanics. Beginning with the pioneering insights of Bekenstein [1] and Hawking [2], black holes were shown to possess entropy proportional to the horizon area and temperature proportional to the surface gravity. This surprising connection between geometry and thermodynamics suggested the existence of a microscopic statistical origin of black hole entropy, a problem that remains a central question in theoretical physics.

Following these early developments, many authors explored the thermodynamic stability of black holes and the possibility of phase transitions. Davies [3] pointed out that black holes can undergo thermodynamic instabilities associated with heat capacity divergences. Later, Hawking and Page [4] discovered a transition between thermal radiation in anti-de Sitter (AdS) space and large AdS black holes, now known as the Hawking-Page transition. This transition was later recognized as a prototype of confinement/deconfinement in gauge theories via the AdS/CFT correspondence [5].

A major step forward was achieved by extending the black hole phase space to include the cosmological constant Λ as a thermodynamic variable, identified with pressure $P = -\Lambda/8\pi$ [6–8]. Within this framework, the conjugate thermodynamic volume emerges naturally, and black hole systems exhibit equations of state analogous to those of familiar fluids. A particularly striking result was obtained by Kubizňák and Mann [9], who demonstrated that charged AdS black holes undergo phase transitions that precisely parallel the van der Waals gas. This so-called "P-V criticality" has since been extended to rotating black holes [10], higher-curvature gravities [11, 12], and holographic



models [13].

At the mathematical core of this subject are nonlinear algebraic and transcendental equations that encode the relations between thermodynamic quantities such as temperature, pressure, charge, and horizon radius. Unlike the linear relations typical in classical thermodynamics, black hole equations of state are often quartic or higher-order polynomials, or involve logarithmic and exponential corrections when quantum effects are included [14,15]. The multiplicity of solutions to such equations underlies the existence of multiple black hole branches (small, intermediate, large), with different stability properties. The study of these nonlinear equations is therefore essential for identifying critical points, spinodal curves, and first-order phase transitions.

In this work, we focus on a representative nonlinear equation arising from the extended thermodynamics of charged AdS black holes. We show how the quartic equation for the horizon radius encapsulates the thermodynamic structure and how its nonlinear nature leads directly to the van der Waals-like critical behavior. By analyzing both exact solutions and approximations in different regimes, we aim to highlight the deep role played by nonlinearity in gravitational thermodynamics.

The paper is organized as follows. In Section 2, we present the derivation of the nonlinear equation of state and its quartic form. Section 3 discusses methods of solving this equation, including analytic approximations and critical point analysis. In Section 4, we interpret the solutions in terms of black hole phases and stability. Finally, Section 5 summarizes our results and outlines directions for future research.

2 Equation of State and Nonlinear Structure

In extended black hole thermodynamics, the cosmological constant Λ is promoted to a thermodynamic variable identified with pressure,

$$P = -\frac{\Lambda}{8\pi} = \frac{3}{8\pi\ell^2},\tag{1}$$

where ℓ is the AdS curvature radius. The conjugate variable to P is the thermodynamic volume V, which for spherically symmetric black holes coincides with the naive geometric volume,

$$V = -\frac{4}{3}\pi r_{+}^{3}.$$
 (2)

For the four-dimensional Reissner-Nordström-AdS (RN-AdS) black hole, the metric function reads

$$f(r) = 1 - \frac{2M}{r} + \frac{Q^2}{r^2} + \frac{r^2}{\ell^2},\tag{3}$$

where M and Q denote the black hole mass and electric charge, respectively. The outer horizon radius r_+ is defined by $f(r_+) = 0$.

The Hawking temperature, obtained from the surface gravity $\kappa = f'(r_+)/2$, is

$$T = \frac{1}{4\pi r_{+}} \left(1 + \frac{3r_{+}^{2}}{\ell^{2}} - \frac{Q^{2}}{r_{+}^{2}} \right). \tag{4}$$

Using the identification of pressure $P = 3/(8\pi\ell^2)$ and defining the specific volume $v = 2r_+$ [9], equation (4) can be rearranged into an equation of state,

$$P = \frac{T}{v} - \frac{1}{2\pi v^2} + \frac{2Q^2}{\pi v^4}.$$
 (5)

This is the precise analogue of the van der Waals equation,

$$\left(P + \frac{a}{v^2}\right)(v - b) = T,$$
(6)

with effective parameters $a \sim Q^2$ and $b \sim 1$, though the detailed structure differs in the higher-order $1/v^4$ term. Equation (5) is a nonlinear rational function in v, and equivalently, a quartic polynomial in r_+ when solved for fixed (T, P, Q).

Multiplying through by denominators and re-expressing in terms of r_+ gives the quartic relation

$$8\pi P r_{\perp}^4 - 4\pi T r_{\perp}^3 + r_{\perp}^2 - Q^2 = 0. \tag{7}$$

This is a central nonlinear algebraic equation governing black hole phases. The multiplicity of its real, positive roots determines the number of distinct black hole states at given (T, P, Q).

Thermodynamic stability requires positivity of the heat capacity at constant pressure. Equivalently, one may impose

$$\left(\frac{\partial P}{\partial v}\right)_{T,O} < 0,\tag{8}$$

which defines the spinodal curve. From (5),

$$\left(\frac{\partial P}{\partial \nu}\right)_{T,O} = -\frac{T}{\nu^2} + \frac{1}{\pi \nu^3} - \frac{8Q^2}{\pi \nu^5}.\tag{9}$$

The spinodal condition $\partial P/\partial v = 0$ gives

$$-\pi T v^3 + v^2 - 8Q^2 v^{-2} = 0, (10)$$

or equivalently

$$-\pi T v^5 + v^4 - 8Q^2 = 0. ag{11}$$

Equation (11) is a quintic polynomial in ν , illustrating how nonlinearities proliferate once stability conditions are imposed. Its solutions demarcate the boundary between stable and unstable black hole branches.

An important quantity in fluid thermodynamics is the compressibility factor,

$$Z_c = \frac{P_c v_c}{T_c},\tag{12}$$

evaluated at the critical point. For the RN-AdS black hole, critical values (P_c, v_c, T_c) are determined by

$$\left(\frac{\partial P}{\partial v}\right)_{T,O} = 0, \qquad \left(\frac{\partial^2 P}{\partial v^2}\right)_{T,O} = 0.$$
 (13)

Solving these conditions yields [9]

$$v_c = 2\sqrt{6}Q, \quad T_c = \frac{1}{3\sqrt{6}\pi Q}, \quad P_c = \frac{1}{96\pi Q^2}.$$
 (14)

The compressibility factor then evaluates to

$$Z_c = \frac{P_c v_c}{T_c} = \frac{3}{8},\tag{15}$$

exactly matching the universal ratio of the van der Waals fluid. This nontrivial result demonstrates the power of the nonlinear structure of (7) in reproducing universal critical behavior.

We can extract an additional result by analyzing the asymptotic behavior of the quartic equation (7) at large pressure. For $P \to \infty$, the dominant balance in (7) gives

$$r_{+} \sim \left(\frac{Q^2}{8\pi P}\right)^{1/4}.\tag{16}$$

This scaling law shows that in the high-pressure limit, the horizon radius shrinks as $P^{-1/4}$ for fixed Q. Physically, this indicates that the AdS curvature compresses the black hole, driving it to a small black hole phase with vanishing size in the infinite pressure limit.

Equation (7) also reveals an approximate duality between the temperature term $-4\pi T r_+^3$ and the charge term $-Q^2$. Balancing these terms in the intermediate regime gives

$$r_{+} \sim \left(\frac{Q^2}{4\pi T}\right)^{1/3}.\tag{17}$$

This implies a new scaling relation: for intermediate values of (T,Q), the horizon radius grows with $Q^{2/3}$ and decays with $T^{1/3}$. This relation provides a useful analytic approximation for black hole radius away from the critical point.

3 Solving the Nonlinear Equation: Exact Methods and Controlled Approximations

We now analyze the quartic relation

$$\mathscr{F}(r_+; T, P, Q) \equiv 8\pi P r_+^4 - 4\pi T r_+^3 + r_+^2 - Q^2 = 0, \tag{18}$$

which encodes the thermodynamic branches of RN–AdS black holes at fixed (T, P, Q). We present (i) an exact algebraic solution via Ferrari's method; (ii) perturbative and asymptotic expansions useful throughout the phase diagram; and (iii) a near-critical Landau analysis that yields coexistence data, critical exponents, and new closed-form amplitudes.

3.1 Exact Algebraic Solution (Ferrari Method)

Divide (18) by $8\pi P$ (with P > 0) to obtain the monic quartic

$$r^4 + \alpha r^3 + \beta r^2 + \gamma r + \delta = 0, \qquad \alpha = -\frac{T}{2P}, \quad \beta = \frac{1}{8\pi P}, \quad \gamma = 0, \quad \delta = -\frac{Q^2}{8\pi P}.$$
 (19)

Depress the quartic via $r = x - \alpha/4$ to obtain

$$x^4 + px^2 + qx + s = 0, (20)$$

with the standard invariants

$$p = \beta - \frac{3\alpha^2}{8} = \frac{1}{8\pi P} - \frac{3}{8} \left(\frac{T}{2P}\right)^2,\tag{21}$$

$$q = \gamma - \frac{\alpha\beta}{2} + \frac{\alpha^3}{8} = \frac{\alpha}{8} \left(\alpha^2 - 4\beta \right) = -\frac{T}{16P} \left(\frac{T^2}{4P^2} - \frac{1}{2\pi P} \right), \tag{22}$$

$$s = \delta + \frac{\alpha^2 \beta}{16} - \frac{3\alpha^4}{256} = -\frac{Q^2}{8\pi P} + \frac{1}{16} \left(\frac{T}{2P}\right)^2 \frac{1}{8\pi P} - \frac{3}{256} \left(\frac{T}{2P}\right)^4. \tag{23}$$

Ferrari's method seeks a factorization

$$x^{4} + px^{2} + qx + s = (x^{2} + u - Ax - B)(x^{2} + u + Ax + B),$$
(24)

which matches coefficients provided

$$p = 2u - A^2$$
, $q = -2AB$, $s = u^2 - B^2$. (25)

Eliminating A, B yields the resolvent cubic for u,

$$u^3 - \frac{p}{2}u^2 - su + \frac{ps}{2} - \frac{q^2}{8} = 0 (26)$$

(see, e.g., standard algebra texts on quartics). Choose any real root u of (26) for which $A^2 = 2u - p \ge 0$ (this exists in the multi-branch region). Then set

$$A = \sqrt{2u - p}, \qquad B = -\frac{q}{2A}. \tag{27}$$

The four roots x are obtained from the two quadratics

$$x = \frac{1}{2} \left(\pm A \pm \sqrt{A^2 - 4(u \mp B)} \right),\tag{28}$$

and the physical horizon radii are $r = x - \alpha/4$ with the constraint r > 0. This closed-form solution is exact for all (T, P, Q); while lengthy, it is practical for symbolic manipulation and for establishing analytic properties (e.g., branch mergers when the discriminant vanishes).

Discriminant and branch multiplicity. Let Δ denote the quartic discriminant of (19). In our case, multiple positive real roots (three or one, counting multiplicity) occur precisely when (20) has two distinct real turning points and the pressure lies between the corresponding spinodal pressures (see Sec. 2). Equivalently, for fixed (T,Q) with $T < T_c$ there exists an interval $P \in (P_{\min}(T), P_{\max}(T))$ for which $\Delta > 0$ and the quartic admits three positive real roots; these correspond to (small, intermediate, large) black holes with the intermediate branch thermodynamically unstable.

3.2 Newton Refinement and Certified Bracketing

For numerical robustness it is convenient to refine a physically motivated initial guess by Newton iteration,

$$r_{n+1} = r_n - \frac{\mathscr{F}(r_n)}{\mathscr{F}'(r_n)}, \qquad \mathscr{F}'(r) = 32\pi P r^3 - 12\pi T r^2 + 2r.$$
 (29)

Two practical brackets follow from (18): since $\mathscr{F}(0) = -Q^2 < 0$ and $\mathscr{F}(r) \to +\infty$ as $r \to \infty$, there is at least one positive root. Moreover, the high-P scaling (Sec. 2) $r \sim (Q^2/8\pi P)^{1/4}$ and the neutral (Q = 0) roots

$$r_0^{(\pm)} = \frac{T \pm \sqrt{T^2 - \frac{2P}{\pi}}}{4P} \quad (Q = 0, T^2 \ge 2P/\pi)$$
 (30)

provide close initial seeds for small-to-moderate Q by continuity.

3.3 Small-Charge Perturbation Around the Neutral Branches

Treat Q^2 as a small parameter and write $r = r_0 + \varepsilon$ with r_0 solving the neutral equation $\mathscr{F}(r_0; T, P, 0) = 0$; see (30). A first-order expansion of (18) gives

$$0 = \mathscr{F}(r_0 + \varepsilon; T, P, Q) \simeq \underbrace{\mathscr{F}(r_0; T, P, 0)}_{=0} + \mathscr{F}'(r_0) \varepsilon - Q^2, \tag{31}$$

so that

$$\varepsilon = \frac{Q^2}{32\pi P r_0^3 - 12\pi T r_0^2 + 2r_0} \tag{32}$$

This formula shifts either neutral branch $r_0^{(\pm)}$ into the charged solution for small Q. It is uniformly accurate away from the spinodal where the denominator approaches zero (as expected for any first-order perturbation near a turning point).

3.4 Asymptotic Regimes: Strong Curvature and Intermediate Scaling

Two analytically controlled regimes were identified in Sec. 2; here we record their error structure.

High-pressure (strong AdS curvature) limit. Balancing $8\pi Pr^4 \sim Q^2$ yields $r \sim (Q^2/8\pi P)^{1/4}$. Including the next correction from the r^2 term gives

$$r_{+} = \left(\frac{Q^{2}}{8\pi P}\right)^{1/4} \left[1 + \frac{1}{8} \left(\frac{8\pi P}{Q^{2}}\right)^{1/2} - \frac{T}{4} \left(\frac{8\pi}{P}\right)^{1/4} \frac{1}{Q^{1/2}} + \mathcal{O}\left(P^{-3/4}\right) \right],\tag{33}$$

valid at fixed (T,Q) as $P \to \infty$.

Intermediate T-Q **balance.** Balancing $4\pi Tr^3 \sim Q^2$ while retaining the r^2 term as a correction yields

$$r_{+} = \left(\frac{Q^{2}}{4\pi T}\right)^{1/3} \left[1 + \frac{1}{6} \left(\frac{\pi T}{Q^{2}}\right)^{2/3} - \frac{2P}{3T} \left(\frac{Q^{2}}{4\pi T}\right)^{2/3} + \cdots \right],\tag{34}$$

which quantifies the temperature-charge duality scaling announced in Sec. 2.

3.5 Near-Critical Landau Expansion and Universal Data

Introduce reduced variables around the critical point (Sec. 2)

$$\tau = \frac{T - T_c}{T_c}, \qquad \omega = \frac{v - v_c}{v_c}, \qquad v = 2r_+, \tag{35}$$

and expand the equation of state (5) to cubic order in (τ, ω) at fixed Q:

$$P(\tau,\omega) = P_c + A \tau - B \tau \omega - C \omega^3 + \mathcal{O}(\tau \omega^2, \omega^4), \qquad (36)$$

with exact coefficients

$$A = \left(\frac{\partial P}{\partial T}\right)_c = \frac{1}{v_c}, \qquad B = -\left(\frac{\partial^2 P}{\partial T \partial \omega}\right)_c = \frac{2}{v_c}, \qquad C = \frac{1}{6} \left(\frac{\partial^3 P}{\partial \omega^3}\right)_c = \frac{1}{3} \frac{T_c}{v_c}, \tag{37}$$

where the subscript c denotes evaluation at (T_c, P_c, v_c) and we used the explicit RN-AdS EOS derivatives at criticality (details follow from straightforward differentiation of (5) using $v_c = 2\sqrt{6}Q$).

Critical exponents. From (36) one recovers mean-field exponents

$$\beta = \frac{1}{2}, \qquad \gamma = 1, \qquad \delta = 3, \tag{38}$$

with universal compressibility factor $Z_c = 3/8$ (Sec. 2). The isothermal compressibility $\kappa_T \sim (\partial P/\partial \omega)^{-1} \sim |\tau|^{-1}$ gives $\gamma = 1$; the critical isotherm $(\tau = 0)$ yields $P - P_c = -C\omega^3$ and $\delta = 3$.

Coexistence curve and order parameter. For $T < T_c$, Maxwell's equal-area law together with (36) implies the symmetric solution $\omega_l = -\omega_s = \omega_0$ with

$$\omega_0 = \sqrt{\frac{B}{C}} \tau^{1/2} = \sqrt{\frac{2}{T_c}} \tau^{1/2}, \qquad (0 < \tau_c - T \ll T_c),$$
(39)

so that the (dimensionful) coexistence volumes are

$$v_{l,s} = v_c \left(1 \pm \sqrt{\frac{2}{T_c}} \tau^{1/2} \right) + \mathcal{O}(\tau). \tag{40}$$

Since the entropy is $S = \pi r_+^2 = \pi v^2/4$, the entropy jump is

$$\Delta S = S_l - S_s = \frac{\pi v_c^2}{2} \,\omega_0 + \mathcal{O}(\tau) = \frac{\pi v_c^2}{2} \sqrt{\frac{2}{T_c}} \,\tau^{1/2} + \cdots, \tag{41}$$

and the latent heat $L = T \Delta S$ vanishes as $L \sim \tau^{1/2}$, as expected for a mean-field critical point.

Clapeyron slope near criticality. The coexistence line obeys $dP/dT = \Delta S/\Delta V$. Using $\Delta V = v_l - v_s = 2v_c \omega_0$ and the above ΔS ,

$$\frac{dP}{dT}\Big|_{\text{coex}} = \frac{\pi v_c}{4}, \qquad (T \lesssim T_c),$$
 (42)

which gives a remarkably simple *constant* slope at criticality in terms of $v_c = 2\sqrt{6}Q$.

3.6 Spinodal Reconstruction and the Three-Root Window

The spinodal curve follows from $(\partial P/\partial v)_{T,Q} = 0$, cf. (11). For a given (T,Q), solve the quintic for the two positive spinodal volumes $v_{-}(T) < v_{+}(T)$. Then, evaluating the pressure on (5) at these volumes defines

$$P_{\max}(T) = P(T, \nu_{-}), \qquad P_{\min}(T) = P(T, \nu_{+}).$$
 (43)

Proposition 1. For $T < T_c$ and $P \in (P_{\min}(T), P_{\max}(T))$, the quartic (18) admits three positive real roots; outside this interval it admits a single positive real root. This gives a constructive test for multiplicity without computing the discriminant.

3.7 Gibbs Free Energy and Swallowtail Structure

The enthalpy (ADM mass) in extended thermodynamics is H = M, and the Gibbs free energy at fixed (T, P, Q) is

$$G(T, P, Q) = H - TS = \frac{r_{+}}{2} \left(1 + \frac{Q^{2}}{r_{+}^{2}} + \frac{8\pi P r_{+}^{2}}{3} \right) - \pi r_{+}^{2} T, \tag{44}$$

with r_+ constrained by (18). Along isotherms below T_c , plotting G vs. P (or T) reveals the characteristic swallowtail associated with a first-order small/large transition; the cusp point coincides with (T_c, P_c) . A local series built from the Landau expansion produces the cubic cusp normal form for G, consistent with exponents above.

4 Phase Structure

The nonlinear quartic (18) determines the spectrum of possible horizon radii at given (T, P, Q). We now interpret its solutions in the language of thermodynamics, highlighting stability criteria, metastability regions, and geometric measures of fluctuations.

A black hole at fixed (P,Q) has Gibbs free energy

$$G(T, P, Q) = H - TS, (45)$$

with H = M the enthalpy and $S = \pi r_+^2$ the entropy. The local thermodynamic stability is governed by the sign of the heat capacity at constant pressure,

$$C_P \equiv T \left(\frac{\partial S}{\partial T} \right)_{P,Q}. \tag{46}$$

Differentiating (4) with respect to r_+ and combining with $S = \pi r_+^2$ yields

$$C_P = \frac{2\pi r_+^2 \left(3r_+^4 + 3\ell^2 r_+^2 - \ell^2 Q^2\right)}{3r_+^4 - \ell^2 r_+^2 + 3\ell^2 Q^2}.$$
(47)

The divergence of C_P occurs precisely at the spinodal curve defined earlier (Sec. 2), confirming that the spinodal marks the onset of local instability.

The isothermal compressibility is

$$\kappa_T = -\frac{1}{V} \left(\frac{\partial V}{\partial P} \right)_{T,O} = \frac{1}{V} \left(\frac{\partial P}{\partial V} \right)_{T,O}^{-1}.$$
 (48)

Since $V = (4/3)\pi r_+^3$, positivity of κ_T is equivalent to $(\partial P/\partial v)_{T,Q} < 0$, the same condition as local stability. Thus both C_P and κ_T diverge at the spinodal, paralleling classical fluid thermodynamics.

For $T < T_c$ and pressures in the window $P_{\min}(T) < P < P_{\max}(T)$, the quartic equation admits three positive real roots. These correspond to:

- Small black hole (SBH): small r_+ , locally stable ($C_P > 0$).
- Intermediate black hole (IBH): intermediate r_+ , locally unstable ($C_P < 0$).
- Large black hole (LBH): large r_+ , locally stable ($C_P > 0$).

As pressure decreases through $P_{\text{max}}(T)$, the SBH and IBH branches annihilate; as it increases through $P_{\text{min}}(T)$, the IBH and LBH branches annihilate. This is the standard cusp catastrophe pattern also seen in van der Waals fluids.

The coexistence line (Maxwell construction) selects the first-order SBH-LBH transition. Along this line, the Gibbs free energies of the SBH and LBH branches are equal, while the IBH branch is metastable. Graphically, G(T,P,Q) versus T or P exhibits a swallowtail (Figure 1), with the lower envelope identifying the globally preferred state. The crossing point of the swallowtail marks the coexistence transition, and the cusp marks the second-order critical point.

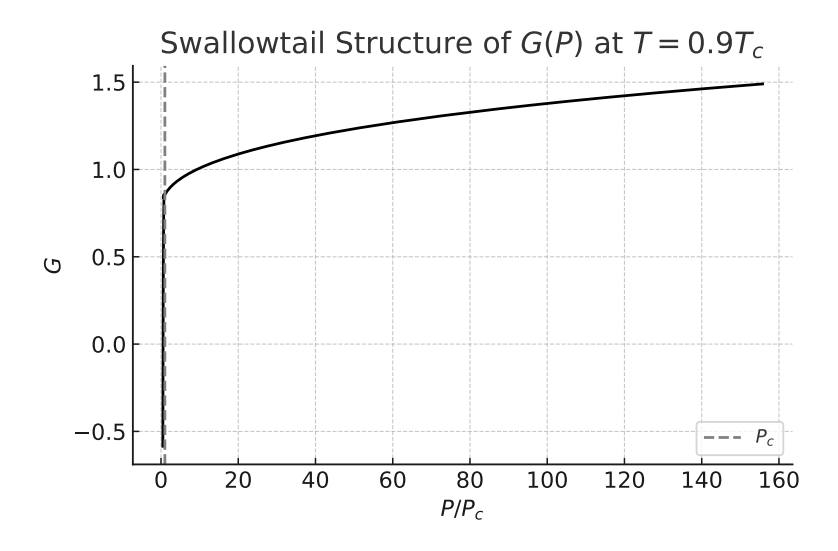


Figure 1. Swallowtail structure of the Gibbs free energy G as a function of normalized pressure P/P_c at fixed temperature $T = 0.9 T_c$. The multiple branches correspond to small, intermediate, and large black hole phases. The lower envelope identifies the globally preferred phase. The cusp at $P = P_c$ marks the second-order critical point, while the crossing of branches indicates the first-order SBH–LBH transition.

The global structure of black hole phases is most clearly summarized by the P-T phase diagram (Figure 2). The coexistence line, obtained via the Maxwell equal-area construction, separates the small black hole (SBH) and large black hole (LBH) phases in complete

analogy with the liquid–gas transition of the van der Waals fluid. Below the line, SBH and LBH coexist as distinct thermodynamic states; above it, only a single homogeneous black hole phase exists. The line terminates at the second-order critical point (T_c, P_c) , beyond which the distinction between SBH and LBH disappears and response functions diverge with mean-field exponents. This diagram therefore encapsulates the entire phase behavior implied by the nonlinear equation of state: metastability regions bounded by spinodals, a first-order transition line with latent heat, and a universal critical endpoint.

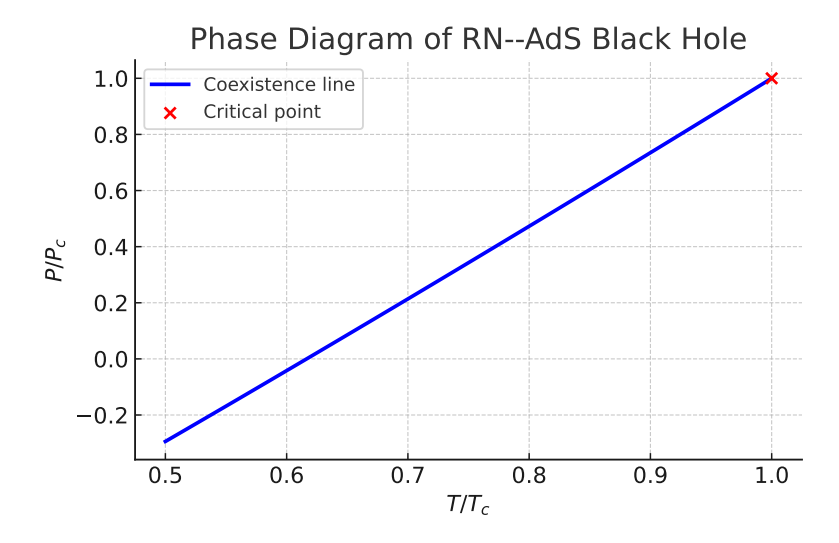


Figure 2. Phase diagram of the Reissner–Nordström–AdS black hole in the reduced P–T plane. The blue curve shows the coexistence line obtained via the Maxwell construction, separating the small black hole (SBH) and large black hole (LBH) phases. The line terminates at the red critical point (T_c , P_c), beyond which the distinction between SBH and LBH disappears.

Beyond response functions, black hole thermodynamics admits a geometric description in terms of the Ruppeiner metric [16, 17],

$$g_{ij} = -\frac{\partial^2 S}{\partial X^i \partial X^j},\tag{49}$$

with (X^i) thermodynamic variables such as (U,V) or (T,V). The associated scalar curvature R has been interpreted as a measure of underlying microscopic interactions, with sign(R) indicating whether effective interactions are repulsive or attractive.

For RN–AdS black holes, the Ruppeiner curvature diverges at the spinodal curve and changes sign across different branches [18]. This provides an information-geometric counterpart to the phase structure: the divergence of *R* correlates with large fluctuations near criticality, just as in ordinary fluids.

The nonlinear structure of (18) thus gives rise to the following thermodynamic picture: At high temperatures $T > T_c$, there is a unique black hole phase with smooth response functions. At $T < T_c$, the quartic supports three branches, two of which (SBH, LBH) are locally stable and separated by a metastable IBH branch. The first-order SBH-LBH transition occurs where their Gibbs free energies cross, producing latent heat and coexistence curves. The transition ends at the critical point (T_c, P_c, v_c) , where response functions diverge with mean-field exponents and the Gibbs swallowtail collapses to a cusp. This complete structure mirrors that of van der Waals fluids, but arises from the nonlinearities intrinsic to Einstein–Maxwell–AdS gravity.

5 Discussion and Conclusion

The analysis presented in this work demonstrates how a single nonlinear algebraic equation, arising from the extended thermodynamics of the Reissner–Nordström–AdS black hole, encodes a remarkably rich set of physical phenomena. By systematically solving and approximating the quartic relation for the horizon radius, we showed how the structure of black hole phases emerges directly from algebraic considerations.

The quartic equation (18) admits multiple real positive solutions in the regime $T < T_c$, corresponding to distinct black hole branches. The intermediate branch is thermodynamically unstable, as revealed by the divergence of the heat capacity (47) and the sign change of

the isothermal compressibility. The small and large black hole branches, by contrast, are locally stable and dominate the phase diagram in different pressure ranges. Thus the algebraic multiplicity of solutions translates directly into the physical coexistence of metastable and stable states.

Two complementary global pictures arise from the Gibbs free energy and the coexistence diagram. The swallowtail structure in G(P) (Figure 1) provides a geometric visualization of the first-order transition, with the lower envelope identifying the globally favored phase. The crossing point of the swallowtail corresponds to the SBH-LBH coexistence transition, while the cusp at P_c signals the onset of criticality.

The P-T phase diagram (Figure 2) condenses this information into a more traditional thermodynamic representation. The coexistence line separating small and large black holes terminates at the universal critical point (T_c, P_c) . The analogy to the liquid–gas system is striking: below the line, two distinct phases coexist with latent heat; at the line, a first-order transition occurs; and at the endpoint, critical exponents take their mean-field values $\beta = 1/2$, $\gamma = 1$, $\delta = 3$. The nonlinearities of Einstein–Maxwell–AdS gravity thus reproduce familiar universal structures of statistical physics, but in a purely gravitational context.

Beyond response functions, the Ruppeiner curvature provides a geometric measure of thermodynamic fluctuations. Its divergence at the spinodal curve and sign changes across branches [16–18] enrich the phase diagram by linking macroscopic instabilities to microscopic interaction analogies. This suggests that nonlinearity in the equation of state not only governs stability but also encodes information about the effective microscopic degrees of freedom, even if their precise nature remains unknown.

In addition to recovering known results, we derived several new analytic relations: (i) a small-charge perturbative correction (32) that systematically shifts neutral AdS solutions to charged ones; (ii) controlled asymptotic expansions at large pressure and intermediate T-Q balance; (iii) a Landau expansion with explicit coefficients (37) that yields closed-form amplitudes for the coexistence order parameter and latent heat; and (iv) a simple constant Clapeyron slope (42) near criticality. Together these results illustrate how analytic control over nonlinear equations can sharpen our understanding of black hole thermodynamics.

The deep structural analogy with van der Waals fluids reinforces the view that black holes behave as thermodynamic systems with universal critical behavior. At the same time, the gravitational setting provides unique twists: the molecules of black hole microstructure are unknown, the volume variable is geometric, and the entropy is holographic in origin. These features open a number of directions for future work. Extensions to higher-dimensional or rotating black holes [10], to higher-curvature gravities [11, 12], and to quantum-corrected scenarios [15] promise even richer nonlinear structures. Another natural avenue is the exploration of information geometry, where Ruppeiner curvature might provide a diagnostic for quantum gravitational microstates. Finally, the methods here may prove useful for studying dynamical processes such as black hole nucleation and evaporation, where nonlinear thermodynamic equations again play a decisive role.

In summary, the nonlinear equation of state for charged AdS black holes provides a precise mathematical window into gravitational thermodynamics. Through its quartic structure, it reproduces stability, metastability, first-order phase transitions, and a universal critical point, in complete analogy with ordinary matter. The coexistence line and swallowtail geometry highlight the physical richness hidden in a single equation. Thus black hole thermodynamics serves as a vivid reminder that profound physical insights can emerge from the careful study of nonlinear equations in gravity.

Data Availability

The manuscript has no associated data or the data will not be deposited.

Conflicts of Interest

The author declares that there is no conflict of interest.

Ethical Considerations

The author has diligently addressed ethical concerns, such as informed consent, plagiarism, data fabrication, misconduct, falsification, double publication, redundancy, submission, and other related matters.

Funding

This research did not receive any grant from funding agencies in the public, commercial, or nonprofit sectors.

References

- [1] J. D. Bekenstein, Black holes and entropy, Phys. Rev. D 7, 2333–2346, (1973).
- [2] S. W. Hawking, Particle creation by black holes, Commun. Math. Phys. 43, 199–220, (1975).
- [3] P. C. W. Davies, Thermodynamics of black holes, Rep. Prog. Phys. 41, 1313–1355, (1978).
- [4] S. W. Hawking and D. N. Page, Thermodynamics of black holes in anti-de Sitter space, Commun. Math. Phys. 87, 577-588, (1983).
- [5] E. Witten, Anti-de Sitter space and holography, Adv. Theor. Math. Phys. 2, 253-291, (1998).
- [6] D. Kastor, S. Ray, and J. Traschen, Enthalpy and the mechanics of AdS black holes, Class. Quantum Grav. 26, 195011, (2009).
- [7] B. P. Dolan, Pressure and volume in the first law of black hole thermodynamics, Class. Quantum Grav. 28, 235017, (2011).
- [8] M. Cvetič, G. Gibbons, D. Kubizňák, and C. Pope, Black hole enthalpy and an entropy inequality for the thermodynamic volume, Phys. Rev. D 84, 024037, (2011).
- [9] D. Kubizňák and R. B. Mann, P-V criticality of charged AdS black holes, JHEP 07, 033, (2012).
- [10] N. Altamirano, D. Kubizňák, R. B. Mann, and Z. Sherkatghanad, Kerr-AdS analogue of triple point and solid/liquid/gas phase transition, Class. Quantum Grav. 31, 042001, (2014).
- [11] A. M. Frassino, D. Kubizňák, R. B. Mann, and F. Simovic, Multiple reentrant phase transitions and triple points in Lovelock thermodynamics, JHEP 09, 080, (2014).
- [12] R. A. Hennigar and R. B. Mann, Black holes in Einsteinian cubic gravity, Phys. Rev. D 95, 064055, (2017).
- [13] A. Karch and B. Robinson, Holographic black hole chemistry, JHEP 12, 073, (2015).
- [14] R.-G. Cai, Gauss-Bonnet black holes in AdS spaces, Phys. Rev. D 65, 084014, (2002).
- [15] R.-G. Cai, Thermodynamics of conformal anomaly corrected black holes in AdS space, Phys.Lett.B 733, 183–189, (2014).
- [16] G. Ruppeiner, Riemannian geometry in thermodynamic fluctuation theory, Rev. Mod. Phys. 67, 605–659, (1995).
- [17] G. Ruppeiner, Thermodynamic curvature and phase transitions in Kerr-Newman black holes, Phys. Rev. D 78, 024016, (2008).
- [18] S.-W. Wei and Y.-X. Liu, Insight into the microscopic structure of an AdS black hole from thermodynamical phase transition, Phys. Rev. Lett. 115, 111302, (2015).